

1 **Supporting Information**

2
3 **Viscosity of erythritol and erythritol-water particles as a function of water activity: new results**
4 **and an intercomparison of techniques for measuring the viscosity of particles**

5
6 **Yangxi Chu^{1,a}, Erin Evoy^{2,a}, Saeid Kamal², Young Chul Song³, Jonathan P. Reid³, Chak K.**
7 **Chan¹ and Allan K. Bertram²**

8 ¹School of Energy and Environment, City University of Hong Kong, 83 Tat Chee Avenue, Kowloon,
9 Hong Kong, China

10 ²Department of Chemistry, University of British Columbia, 2036 Main Mall, Vancouver, BC, V6T
11 1Z1, Canada

12 ³School of Chemistry, University of Bristol, Bristol, BS8 1TS, United Kingdom

13
14 ^aThese authors contributed equally to this work.

15
16 **Correspondence:** Allan K. Bertram (bertram@chem.ubc.ca)

17

18 **S1. Calculation of conditioning times for droplets**

19 To determine the time needed for conditioning droplets to a known water activity (a_w), we first
20 estimated the characteristic time for the diffusion of water molecules within erythritol-water droplets
21 (τ_w) using the following equation (Seinfeld and Pandis, 2006; Shiraiwa et al., 2011):

$$\tau_w = r_p^2 / (\pi^2 D_w), \quad (\text{S1})$$

22 where r_p is the droplet radius and D_w is the diffusion coefficient of water within the droplet. τ_w in
23 Eq. (S1) is the time when the concentration of water at the droplet center deviates by less than a
24 factor of $1/e$ from the equilibrated value. To estimate D_w , we first estimated the upper limit of the
25 viscosity of erythritol droplets using Table SI.22 in Song et al. (2016). Next, we converted the
26 viscosity to a_w using Table S2 in Marshall et al. (2016). Finally, we converted the a_w to D_w using
27 Table 1 and Eq. (4) in Price et al. (2014). This procedure assumes that the D_w values are identical
28 for erythritol-water and sucrose-water particles having the same viscosity.

29 In our experiments, a duration of at least $6.5 \tau_w$ was allowed for conditioning to a certain a_w (Table
30 S1). Section 3.2 in the main text shows that this duration is sufficient for particles to equilibrate with
31 the corresponding relative humidity in the surrounding gas phase.

32

33 **S2. Fluorescence intensity as a function of RBID mass fraction in conditioned thin film**

34 Prior to rFRAP experiments, we measured the average fluorescence intensity as a function of RBID
35 concentration in sample films with $a_w = 0.630 \pm 0.025$. The fluorescence intensity was averaged
36 over an area of approximately $30 \times 30 \mu\text{m}^2$. The laser scanning microscope settings used were
37 identical to those in Sect. 2.1.2 in the main text. Figure S2 shows the average fluorescence intensity
38 as a function of the mass fraction of RBID. The average fluorescence intensity was linearly
39 proportional to the mass fraction of RBID in sample films in the range of 0–2 weight percent. rFRAP
40 experiments were performed using RBID concentrations within this range.

41

42 **S3. Effect of reversible photobleaching on fluorescence recovery in rFRAP experiments**

43 To determine if processes besides diffusion were responsible for the recovery of fluorescence in the
44 photobleached region, a series of experiments with small droplets (10–30 μm in diameter)
45 containing erythritol, water, and trace amount of RBID (approximately 0.3 weight percent) was
46 carried out. In these experiments, we uniformly photobleached the entire droplet, resulting in $\sim 30\%$
47 reduction in fluorescence intensity. Uniform bleaching ensures that the diffusion of fluorescent
48 RBID molecules will not result in a change in fluorescence intensity. After bleaching, the average
49 fluorescence intensity of the entire droplet was monitored over time, as shown in Fig. S3. The
50 fluorescence intensity remained constant within the uncertainty of the measurements, indicating that
51 reversible photobleaching did not occur on the time scale of our rFRAP experiments.

52

53 **Tables**

54 **Table S1.** Experimental parameters used when conditioning the erythritol-water droplets to a known
 55 water activity (a_w) prior to the rFRAP experiments.

a_w	Droplet radius (μm)	τ_w at a_w lower limit ^a	Actual conditioning time
0.019 ± 0.019	100	3.3 h	80 h
0.023 ± 0.023	100	3.3 h	24 h
0.047 ± 0.047	100	3.3 h	21.5 h
0.053 ± 0.053	100	3.3 h	48 h
0.050 ± 0.050	100	3.3 h	72 h
0.048 ± 0.048	100	3.3 h	96 h
0.261 ± 0.025	150	1.7 h	48 h
0.514 ± 0.025	170	0.41 h	68 h

56 ^a τ_w is the calculated characteristic time for water molecules to diffuse within erythritol-water
 57 droplets of specified radii at the lower limit of a_w , corresponding to the upper limit of droplet
 58 viscosity.

59

60 **Table S2.** Results from rFRAP experiments.

a_w	RBID diffusion coefficients ($\text{m}^2 \text{s}^{-1}$) ^a			Viscosity of erythritol-water particles (Pa s)		
	Mean	Upper limit	Lower limit	Mean	Upper limit	Lower limit
0.019 ± 0.019	1.19×10^{-15}	1.63×10^{-15}	8.67×10^{-16}	30.7	42.1	22.4
0.023 ± 0.023	3.35×10^{-15}	4.17×10^{-15}	2.69×10^{-15}	10.9	13.5	8.75
0.047 ± 0.047	1.47×10^{-15}	3.43×10^{-15}	6.29×10^{-16}	24.7	57.7	10.6
0.053 ± 0.053	2.76×10^{-15}	4.81×10^{-15}	1.58×10^{-15}	13.2	22.9	7.54
0.050 ± 0.050	2.36×10^{-15}	4.12×10^{-15}	1.35×10^{-15}	15.4	26.9	8.80
0.048 ± 0.048	6.36×10^{-15}	1.00×10^{-14}	4.05×10^{-15}	5.71	8.97	3.63
0.261 ± 0.025	1.67×10^{-14}	2.21×10^{-14}	1.27×10^{-14}	2.18	2.88	1.65
0.514 ± 0.025	2.86×10^{-13}	3.52×10^{-13}	2.33×10^{-13}	0.127	0.157	0.104

61 ^aThe reported RBID diffusion coefficients are the result of a minimum of four repeated
62 measurements on separate thin films.

63

64 **Table S3.** Viscosity of erythritol at $a_w < 0.1$ measured using the optical tweezer technique in this
 65 study.

a_w	\log_{10} (viscosity / Pa s)	Viscosity (Pa s) of erythritol-water particles			Method
		Mean	Upper limit	Lower limit	
0.040 ± 0.020	3.04 ± 0.92	1.10×10^3	9.12×10^3	1.32×10^2	Brightfield imaging
0.085 ± 0.020	2.32 ± 1.68	2.09×10^2	1.00×10^4	4.37×10^0	Brightfield imaging

66

67

68 **Table S4. Literature viscosity data included in Fig. 9 in the main text.**

Class	Compound	Viscosity (Pa s)	Reference
Alkane	n-butane	$1.8 \times 10^{-4}{}^a$	Rothfuss and Petters (2017)
Alcohol	1-butanol	$2.9 \times 10^{-3}{}^a$	Rothfuss and Petters (2017)
	2-butanol	$3.7 \times 10^{-3}{}^a$	Rothfuss and Petters (2017)
Diol	1,2-butanediol	$6.6 \times 10^{-2}{}^a$	Rothfuss and Petters (2017)
	1,4-butanediol	$9.1 \times 10^{-2}{}^a$	Rothfuss and Petters (2017)
	2,3-butanediol	$1.3 \times 10^{-1}{}^a$	Rothfuss and Petters (2017)
Triol	1,2,3-butanetriol	1.6×10^0 (1.5×10^0 – 1.7×10^0) ^b	Grayson et al. (2017)
	1,2,4-butanetriol	1.8×10^0 (1.0×10^0 – 3.1×10^0) ^a	Song et al. (2016)

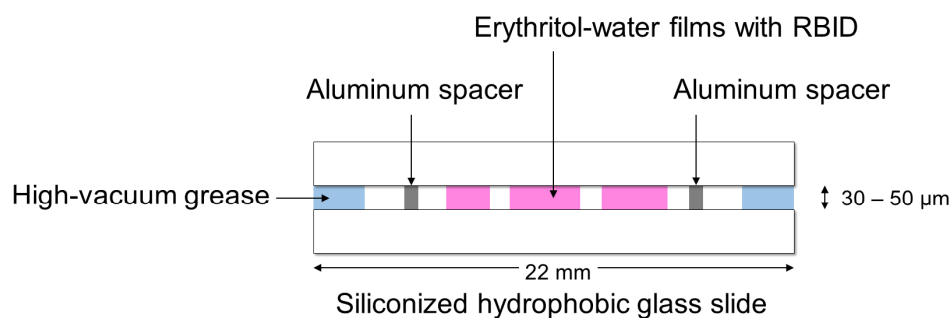
69 ^aViscosity data at 293 K were estimated using the parameterization of viscosity as a function of
70 temperature given in specified references.

71 ^bMeasurement was performed at 295 K using a rotational rheometer.

72

Figures

(a) Side view



(b) Top view

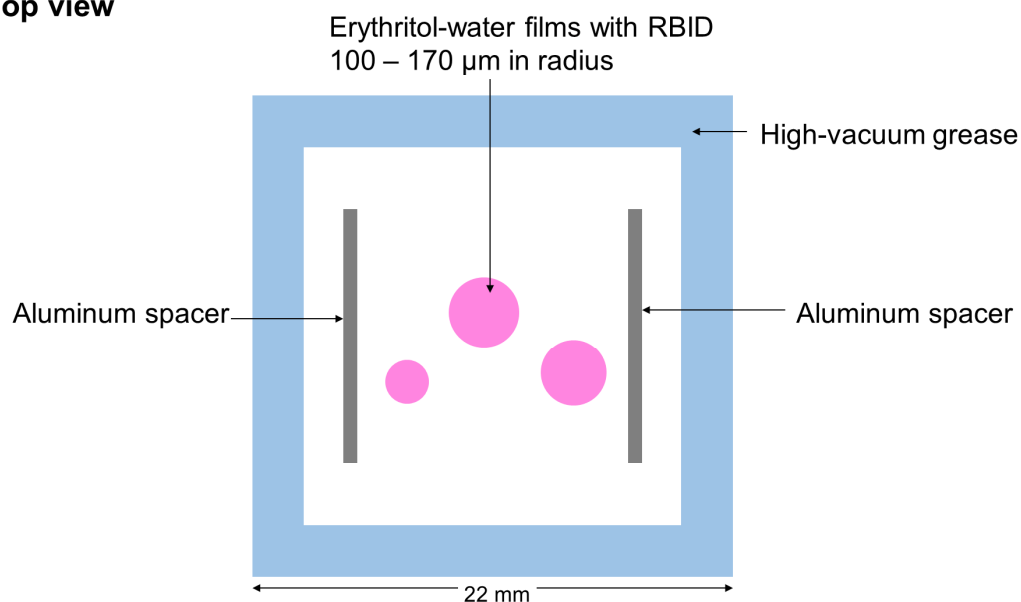


Figure S1. (a) Side view and (b) top view of thin films containing erythritol, water and trace amounts of RBID as the fluorescent dye. The films were sandwiched between two siliconized hydrophobic glass slides for rFRAP experiments. A pair of aluminum spacers were placed between the slides to create films with a thickness of 30–50 μm.

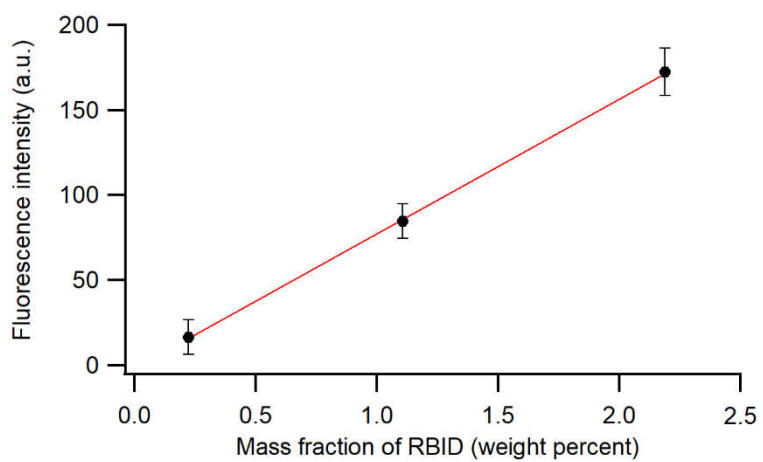


Figure S2. Average fluorescence intensity as a function of RBID mass fraction in sample films at $a_w = 0.630 \pm 0.025$. The red line is a linear fit to the data. Error bars represent two standard deviations of the fluorescence intensity.

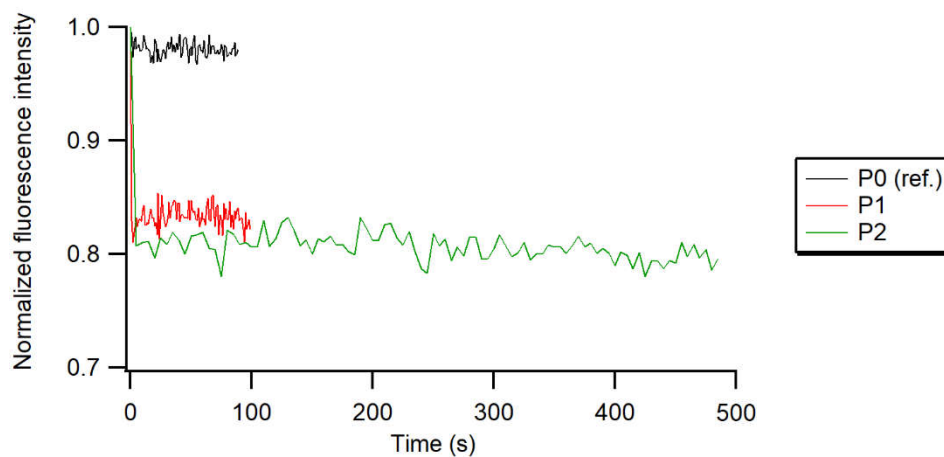


Figure S3. Average fluorescence intensity as a function of time following the uniform photobleaching of an entire droplet. The average fluorescence intensities after photobleaching were normalized against an image taken prior to photobleaching. The RBID mass fractions within the conditioned droplets was approximately 0.3 weight percent. P0 represents a non-photobleached reference droplet. P1 and P2 represent two droplets chosen for the experiments.

References

- Grayson, J. W., Evoy, E., Song, M., Chu, Y., Maclean, A., Nguyen, A., Upshur, M. A., Ebrahimi, M., Chan, C. K., Geiger, F. M., Thomson, R. J. and Bertram, A. K.: The effect of hydroxyl functional groups and molar mass on the viscosity of non-crystalline organic and organic–water particles, *Atmos. Chem. Phys.*, 17(13), 8509–8524, doi:10.5194/acp-17-8509-2017, 2017.
- Marshall, F. H., Miles, R. E. H., Song, Y.-C., Ohm, P. B., Power, R. M., Reid, J. P. and Dutcher, C. S.: Diffusion and reactivity in ultraviscous aerosol and the correlation with particle viscosity, *Chem. Sci.*, 7(2), 1298–1308, doi:10.1039/C5SC03223G, 2016.
- Price, H. C., Murray, B. J., Mattsson, J., O’Sullivan, D., Wilson, T. W., Baustian, K. J. and Benning, L. G.: Quantifying water diffusion in high-viscosity and glassy aqueous solutions using a Raman isotope tracer method, *Atmos. Chem. Phys.*, 14(8), 3817–3830, doi:10.5194/acp-14-3817-2014, 2014.
- Rothfuss, N. E. and Petters, M. D.: Influence of Functional Groups on the Viscosity of Organic Aerosol, *Environ. Sci. Technol.*, 51(1), 271–279, doi:10.1021/acs.est.6b04478, 2017.
- Seinfeld, J. H. and Pandis, S. N.: *Atmospheric Chemistry and Physics: From Air Pollution to Climate Change*, 2nd Edition, Wiley., 2006.
- Shiraiwa, M., Ammann, M., Koop, T. and Poschl, U.: Gas uptake and chemical aging of semisolid organic aerosol particles, *Proc. Natl. Acad. Sci.*, 108(27), 11003–11008, doi:10.1073/pnas.1103045108, 2011.
- Song, Y. C., Haddrell, A. E., Bzdek, B. R., Reid, J. P., Bannan, T., Topping, D. O., Percival, C. and Cai, C.: Measurements and Predictions of Binary Component Aerosol Particle Viscosity, *J. Phys. Chem. A*, 120(41), 8123–8137, doi:10.1021/acs.jpca.6b07835, 2016.